

Design and application of two-stage batch mode on methylene blue removal from solution by activated carbon for optimization of adsorbent consumption

Ruize Zhang, Kang Wen, Runping Han*

College of Chemistry, Zhengzhou University, No. 100 of Kexue Road, Zhengzhou 450001, China, Tel. +86 371 67781757; emails: rphan67@zzu.edu.cn (R.P. Han), 690724768@qq.com (R. Zhang), 1039171416@qq.com (K. Wen)

Received 26 March 2020; Accepted 10 July 2020

ABSTRACT

This study focuses on improving the effectiveness of activated carbon (AC) by two-stage batch adsorbing application and calculation of the multi-stage batch adsorption limitation which were compared with the data from experiments. Firstly, the isotherms of methylene blue (MB) adsorption onto AC were presented at 293, 303 and 313 K. Langmuir and Temkin models were performed to obtain the minimal error of fitting. The two-stage batch adsorption model was designed to promote the removal efficiency in fixed adsorbent consumption by a series of functional relation derivation from the isotherm function and mass conservation. For further discussing the situation of more than two adsorption stage, the multi-stage batch adsorption model was developed from two-stage by adsorbent mass approximating treatment and integrating all the single-stage adsorption processes. The results indicated that the increase of removal efficiency from the two-stage batch adsorption got to 5.2% higher, comparing the single-stage batch adsorption process in the initial conditions of 10 mL 500 mg/L MB solution and 10 mg adsorbent mass. Secondly, according to the two-stage batch mode, a series of verified experiments were operated under the same circumstance and the real experimental consequences revealed its validity and reliability. Meanwhile, for achieving the fixed removal efficiency, a series of adsorption simulations were calculated according to the two-stage batch adsorption which showed almost 30% amount of adsorbent was saved for 99% removal efficiency arrival. In addition, the efficient comparison among single, two and multi-stage batch adsorption and economic, practical values of two-stage were further demonstrated.

Keywords: Activated carbon; Adsorption; Methylene blue; Two-stage batch mode; Optimization design

1. Introduction

Recently various kinds of contamination in the water had been witnessed more and more commonly [1]. As the class of main industrial pollution, dyes were often tracked into streams of factories such as paper, food, printing and textile industries [2]. With the demands of these chemical products increasing, these chemicals had caused serious damages to both environment and creatures. In recent years, there were many relative investigations about the removal

of dyes from wastewater through low-cost adsorbents and cost-effective methods [3,4].

Activated carbon (AC) is a carbonaceous, highly porous adsorption medium that has a complex structure composed primarily of carbon atoms. It had been regarded as one of the most efficient solid adsorbents. The carbon materials are well known as their flourishing pore structure, high adsorbing capability, effectiveness and stability [5]. It is no doubt that there is a quite excellent property and various carbon materials have played a significant role in industrial processes. However, the costs of using activated carbon

* Corresponding author.

massively were unacceptable for some low-profit production. Therefore, it is a flaw that gradually grows an obstacle to its further development. Thus, research about increasing the effectiveness of AC has become a hot issue at the moment [6].

Theoretically, as an ideal countercurrent adsorption process, packed-bed adsorption could obviously improve the adsorption capability of adsorbent [7]. But several disadvantages have resisted its further application such as excessive head loss, air blinding, and fouling with particulate matter associated with the fixed-bed adsorption process. Furthermore, packed-bed adsorption is not suitable for the adsorption process of fine AC powder. Comparing with the packed-bed process, there almost no pressure drop caused by the fine size of adsorbent particles in batch adsorption. Additionally, the shaking process has a significant increase of adsorption by reducing mass transfer resistance at the phase interface [8].

As we all know, there have been several isotherms and kinetics models created for describing the process of adsorption. For instance, the common isotherm models include Langmuir, Freundlich and Temkin models which often applied for the description of the chemical or physical adsorbing process. By collecting the experimental data of isotherm and kinetics, the process design and operating conditions optimization was able to be precisely predicted [9]. Previous researches have developed a two-stage batch mode which has been widely applied for the optimization of minimum contact time and a minimum amount of adsorbent, based on isotherm and kinetic models. As the resemble model of extraction, allocating the mass of adsorbent or contact time of adsorption form once to many stages quite benefits to the efficiency improvement of the adsorption process [10].

However, when it comes to practical applications, there was too much contents involved in the theoretical prediction of this model rather than experimental results [11,12]. Therefore, this research focuses on adopting the method of two-stage adsorption model to promote the use ratio of adsorbents and comparison the data between the predicted results and experimental results which was guided to the proper conclusion about the reasonable application of two-stage models.

2. Materials and methods

2.1. Materials

Activated carbon (AR, 200 mesh, powder, Macklin, Shanghai, China), methylene blue (MB) (BS, powder, Kermel, Tianjin, China), deionized water (self-made).

The isoelectric point of AC was 7.09 and the Brunauer–Emmett–Teller (BET) surface area of AC was $1.13 \times 10^3 \text{ m}^2/\text{g}$ measured by the BET method (QuantaChrome NOVA 1000, USA). According to the results of Boehm titration, it showed that the total alkaline and acidic groups of AC surface were 0.0528 and 0.388 mmol/g, respectively.

2.2. Preparation

First of all, some AC powder was transferred to a clean beaker which has added a proper amount of deionized

water and stirred the mixture with a glass stick for 5 min. After 2 h soaking, the mixture was filtered to another vessel and the wet materials were moved to vacuum oven. The drying and degassing process lasts for 4 h at 150°C.

The dye used in the batch experiment was MB. MB formula is $\text{C}_{16}\text{H}_{18}\text{ClN}_3\text{S}\cdot 3\text{H}_2\text{O}$ and has a molecular weight of 373.9 g/mol. MB powder was dissolved into distilled water to prepare a series gradient of reserve solution from concentration 50 to 500 mg/L.

2.3. Characterization

The characteristic functional groups of AC before and after MB adsorption were determined by Fourier-transform infrared spectroscopy (FTIR spectrometer, Nicolet iS50, American). The specific surface area was evaluated based on the BET method (ASAP2420-4MP, American). The morphology of AC was characterized by scanning electron microscopy (SEM, FEI Quanta 200F, Holland).

2.4. Single-stage batch adsorption experiment

The removal of MB from aqueous solution by AC was studied in batch mode. A certain amount of adsorbent (solid mass/solution volume, 1.00 g/L) was added to a 50 mL conical flask, and then 10 mL of MB solution was added at an initial concentration of 500 mg/L (solution pH 7.0). Then the conical flasks were placed in a thermostatic shaker (Guohua Enterprise SHZ-82, China) at 120 rpm. After adsorption, AC was separated from the solution by centrifugation at 3,000 r/min and MB concentration was measured. Referring to the standard curve of MB at the maximum wavelength (665 nm), the concentration of MB in the supernatant was measured and calculated by spectrophotometer [13]. (752, Shanghai Shunyu Hengping Scientific Instrument Co., Ltd., China). The amount of adsorbed dye, Q_e mg/g and removal efficiency of dye, R were calculated by Eq. (1).

$$Q_e = \frac{V(C_0 - C_e)}{m} \quad (1)$$

$$R = \frac{C_0 - C_e}{C_0} \quad (2)$$

where C_0 and C_e are the initial and equilibrium concentrations (mg/L), respectively, V is the volume of dye solution (L) and m is the weight of AC (g).

2.5. Adsorption isotherm fitting

The physical and chemical data at the point of adsorption equilibrium usually were used to evaluate the adsorption capacity of certain materials and applicability of the adsorption process [14–16]. According to the adsorbing amount of adsorbent (Q_e , mg/g) at adsorption equilibrium and the residual concentrations (C_e , mg/L) in the solutions, both two series of data could generate a nonlinear curve to describe the changing tendency of Q_e and C_e at the same temperature [17]. It usually has four common isotherm models applied for the isotherm fitting which were shown in Table 1 [18].

Table 1
Nonlinear forms of common isotherm models

Isotherms	Nonlinear equation ($Q_e = f_{\text{iso}}(C_e)$)
Langmuir	$Q_e = \frac{Q_m K_L C_e}{1 + K_L C_e}$
Freundlich	$Q_e = K_F C_e^{1/n}$
Temkin	$Q_e = A + B \ln C_e$
Koble–Corrigan	$Q_e = \frac{AC_e^n}{1 + BC_e^n}$

2.6. Multi-stage batch adsorption model design

The process of multi-stage batch adsorption was demonstrated as Fig. 1 which also described the numeral principles and equivalent relation of adsorption equilibrium. In the first stage, the V mL solution owned C_0 mg/L as its initial concentration was added into the reactor with M_1 g adsorbent and start doing reaction until the adsorption equilibrium. After the first stage reaction, the mass loss of solute in the residual liquid equal to the increased mass of adsorbent theoretically in case of ignoring the loss of volatilization. Then, the residual liquid with concentration C_1 mg/L was transferred to another reactor for the reaction of the second stage. M_2 g adsorbent was added into the reactor and shaking until the adsorption equilibrium. Following these steps, the adsorption can continue going on until the stage i which makes sure that the concentration of residual liquid got to the aimed removal rate.

After a certain extent of data collection of isotherm experiments, isotherm equations were able to set up through fitting tools precisely. Once rebuild the adsorption process with approximated conditions, the results of experiments were supposed to be predicted fairly precisely [19].

For the once batch process, the adsorbent of M_1 g was added into a conical flask with V (L) volume dye solution of concentration C_0 (mg/L). After a period of time, the adsorption process arrived at the equilibrium and measured the residual concentration of solution C_1 (mg/L). There are two methods that could be applied to calculate the unit adsorption amount Q_1 (mg/g) [20].

Therefore, as the once process, there are two equations existed [21]:

$$Q_1 = f_{\text{iso}}(C_1) \tag{3}$$

$$Q_1 M_1 = V(C_0 - C_1) \tag{4}$$

Combining Eqs. (3) and (4), obtain the following expression.

$$f_{\text{iso}}(C_1) = \frac{V(C_0 - C_1)}{M_1} \tag{5}$$

As for the certain isotherm model $f_{\text{iso}}(C)$, the initial conditions C_0 , V and M_1 , the residual concentration C_1 had been evaluated approximately through Eq. (5) [22].

Thus, it is assumed that allocated the total adsorbent mass M (mg/g) into the amount of flasks (n) and operated them. After the first stage came to the adsorption equilibrium, separated the solution and adsorbent and transfer the solution into the next stage which repeated the same

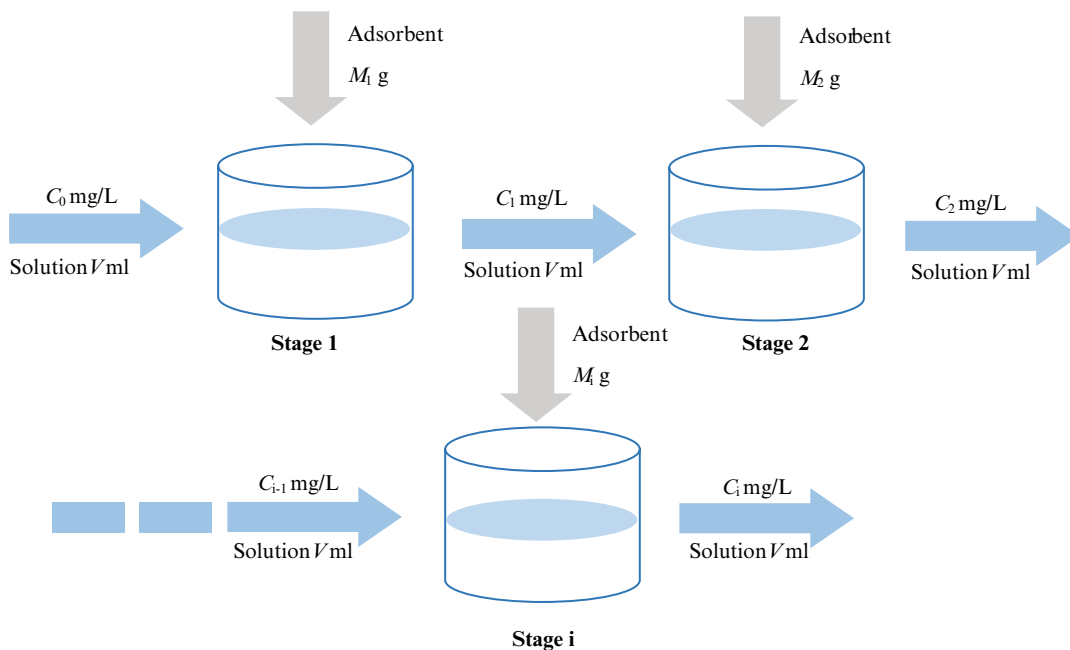


Fig. 1. Multi-stage batch adsorption process for dye removal.

adsorption operation. According to Eq. (5), the quantitative relation between the two contiguous stages was shown as following:

$$C_{i-1} - C_i = \frac{f_{\text{iso}}(C_i)M_i}{V} \quad (6)$$

$$C_0 - C_n = \frac{1}{V} \sum_{i=1}^n f_{\text{iso}}(C_i)M_i \quad (7)$$

$$M = \sum_{i=1}^n M_i \quad (8)$$

Considering the fact that if the value of M_i increased, the C_i will descend obviously. When n approached $+\infty$, M_i was supposed to be enough little. Causing the M was constant, only the M_i approached to 0, the C_i were almost equal to C_{i-1} which means $Q_i (f_{\text{iso}}(C_i))$ was calculated as high as possible. In that case, the left side of Eq. (7) will get to the maximal value. Hence, transfer the Eq. (6) as following:

$$\Delta C = \frac{f_{\text{iso}}(C_i)\Delta M}{V} \quad (9)$$

When the max stage number $n \rightarrow +\infty$, Eq. (9) change to the differential form:

$$dC = \frac{f_{\text{iso}}(C)dM}{V} \quad (10)$$

Consolidated and integrated both sides of Eq. (12):

$$\int_{C_n}^{C_0} \frac{1}{f_{\text{iso}}(C)} dC = \frac{M}{V} \quad (11)$$

In conclusion, the limit value of C_n could be calculated by Eq. (11) and that value was also the maximal value of removal efficiency of the multi-stage adsorption process theoretically [23].

2.7. Two-stage batch adsorption experiment design

In order to alleviate the cost of adsorption, the two-stage batch adsorption experiment was designed for obtaining the highest removal efficiency of MB in the condition of fixed adsorbent consumption. Simply assuming the number of stages only was two ($n = 2$) in Eq. (7), and we ensure the M_1 which means $M_2 = M - M_1$. Besides, the C_0 , V , M and f_{iso} had been confirmed as the known constants.

Firstly, the C_1 could be calculated by Eq. (5):

$$C_1 = g(M_1)_{C_0, V} \quad (12)$$

Then, the result of C_2 will be expressed as:

$$C_2 = g(M_1)_{C_0, V} - \frac{f_{\text{iso}}(C_2)(M - M_1)}{V} \quad (13)$$

In Eq. (13), function $g(M_1)$ represented the relation established by Eqs. (5) and (13). Assuming the initial experimental

conditions were $C_0 = 500$ mg/L, $V = 10$ mg and $M = 10$ mg, the M_1 changed from 2 to 10 mg, and calculated theoretic C_1 and C_2 of the two-stage adsorption process with fitting functions.

For the removal of MB verified experiments in two-stage batch mode, it has to be divided into two processes. In the first step, weight 20 mg adsorbent mass in 50 mL conical flask with 20 mL volume of 500 mg/L MB solution. The next step was to set the well-prepared experimental vessels into the shaker and started the device for 150 min. When the shaking time was over, took out the experimental groups and extracted half volume of solutions which separated from the mixture by centrifuge later and measured the first stage measured concentration $C_{1,m}$. In the second stage of the experiment, the solution obtained from previous vessels was added to another group of vessels with the second batch of adsorbents. After the repeating operations, the final measured concentration $C_{2,m}$ in the supernatant was measured and calculated by spectrophotometer.

2.8. Adsorbent mass optimization of two-stage batch adsorption

In many cases, under the condition of the arrival fixed removal efficiency, the amount of adsorbent could be saved obviously by the two-stage batch operation. When the final removal efficiency R of adsorption process had been set down, the second stage solution concentration C_2 was able to be calculated:

$$C_2 = C_0(1 - R) \quad (14)$$

Causing the M_1 was the known variable, the C_1 could be calculated by Eq. (12), and when M_1 , V , C_1 and C_2 were all settled down, M_2 was obtained by the transformed Eq. (5) as following:

$$M_2 = \frac{V(C_1 - C_2)}{f_{\text{iso}}(M_1)} \quad (15)$$

The final adsorbent consumption of two-stage adsorption M was the sum of M_1 and M_2 . Besides that, due to the final removal efficiency (C_n) known, the theoretic minimal adsorbent consumption was able to be calculated by the multi-stage batch adsorption model Eq. (11). Provided the results of M_1 and M_2 , the total adsorbent mass (M) was plotted to the graph of $M_1 - M$. The initial conditions were assumed as $C_0 = 500$ mg/L, $V = 10$ mL and M_1 increasing from 2 mg and the graphs showed the relation between M_1 and M in case of final R equaling to 90%, 95%, 99% at 293, 303 and 313 K.

3. Results and discussion

3.1. Characterization of AC

Fig. 2 shows the FTIR spectra of AC and MB-loaded AC. The presence of broadband around 3424 cm^{-1} was ascribed to $-\text{OH}$ stretching vibrations due to phenolic or alcoholic functions, while peak around 2918 cm^{-1} was assigned to the $\text{C}-\text{H}$ symmetric and asymmetric vibration mode of methyl and methylene groups [24]. A middle strong bands at 1618 cm^{-1} were ascribed to $\text{C}=\text{C}$ aromatic

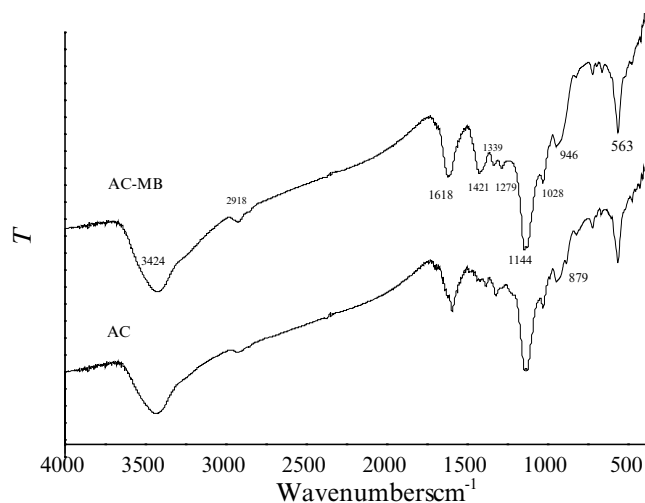


Fig. 2. FTIR analysis of AC and AC-MB.

ring stretching vibration. For MB-loaded AC, it was clearly observed from Fig. 2 that there were four peaks with different intensities located at 1,600; 1,580; 1,500 and 1,450 cm^{-1} , which indicated that the aromatic hydrocarbon skeleton (from MB) increase, and N-CH_3 stretching vibration peaks appear at 1,421 cm^{-1} . After MB adsorption, there were small peaks between 1,279 and 1,421 cm^{-1} that the bands probably were caused by C–N from amide structure. In conclusion, the FTIR results inferred the combination form between AC and MB possibly was covalent bonds.

The adsorption–desorption isotherm of AC on nitrogen was shown in Fig. 3 for BET analysis. The specific surface area was 1,027 m^2/g and the average pore width of aperture adsorption at 4 V/A was 1.79 nm which indicated that AC had a large specific surface area and a large number of pores.

Fig. 4 shows the SEM photographs of AC before (a) and after (b) MB adsorption. The surface of the AC particle became more rough and furry after the adsorption. It was inferred that MB molecular be attracted to the AC surface and occupied the activate sites, besides that too many molecular would also accumulate more than one layer.

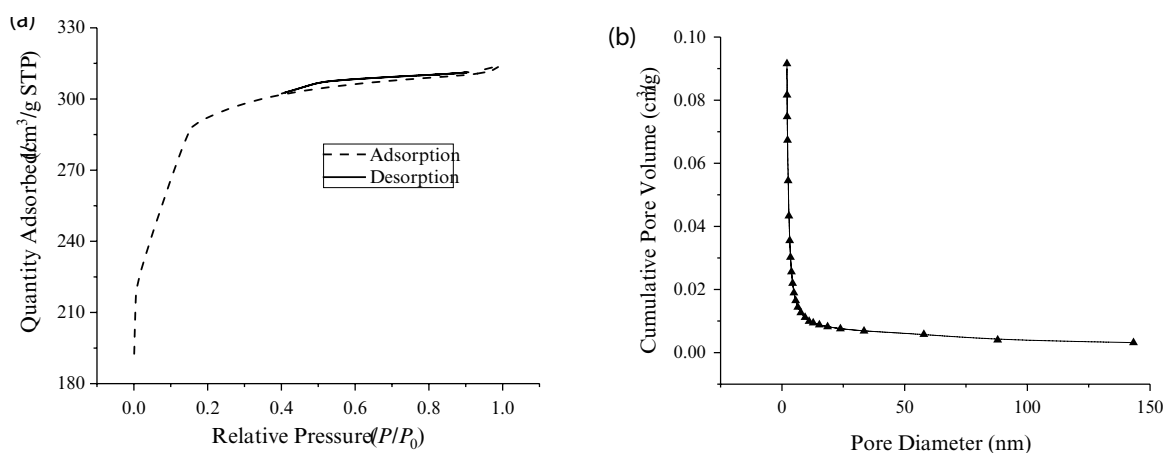


Fig. 3. The nitrogen adsorption and desorption isotherm and pore analysis.

In that case, the mechanism of adsorption AC to MB may be described by Langmuir and the BET adsorption model.

There were more acidic groups (0.388 mmol/g) than basic groups (0.0528 mmol/g) on the surface of the AC [25].

3.2. Adsorption studies

3.2.1. Effect of adsorbent mass on adsorption

In order to study the appropriate adsorbent mass of batch experiments, a series of adsorption experiments were going under the same conditions except for adsorbent mass and the results are shown in Fig. 5. It was clearly noticed from Fig. 5 that the downtrend of unit adsorption amount of AC started slow and steady from the 10 mg adsorbent mass while the removal efficiency was more than 40% which was quite suitable for the subsequent operations at that point.

3.2.2. Effect of contact time on adsorption

Moreover, in order to explore the suitable adsorption time of MB onto AC, a series of different time experimental groups were arranged to study the effect of contact time on adsorption quantity (500 mg/L MB at 303 K). Considering the results of kinetic experiments from Fig. 6, the unit amount of adsorption MB onto AC transferred a dramatic ascending tendency to the steady plateau at a period of 30–150 min. It is evident that the equilibrium of adsorption MB onto AC had already been reached after 150 min.

Through the comprehensive consideration, the relative superior conditions were 10 mg adsorbent mass and 150 min contact time of equilibrium arrival.

3.2.3. Adsorption isotherms

The adsorption isotherms of MB on AC are shown in Fig. 7 at various temperatures. It is noteworthy observed in Fig. 7 that the values of Q_e increased obviously at the range of low concentration with ascending of the concentration, and soon the Q_e gradually approached the maximum unit adsorption amount of AC. The curves started to get a plat and paralleled to x -axis which means the maximal amount of unit adsorption arrived basically. Three curves were fitted

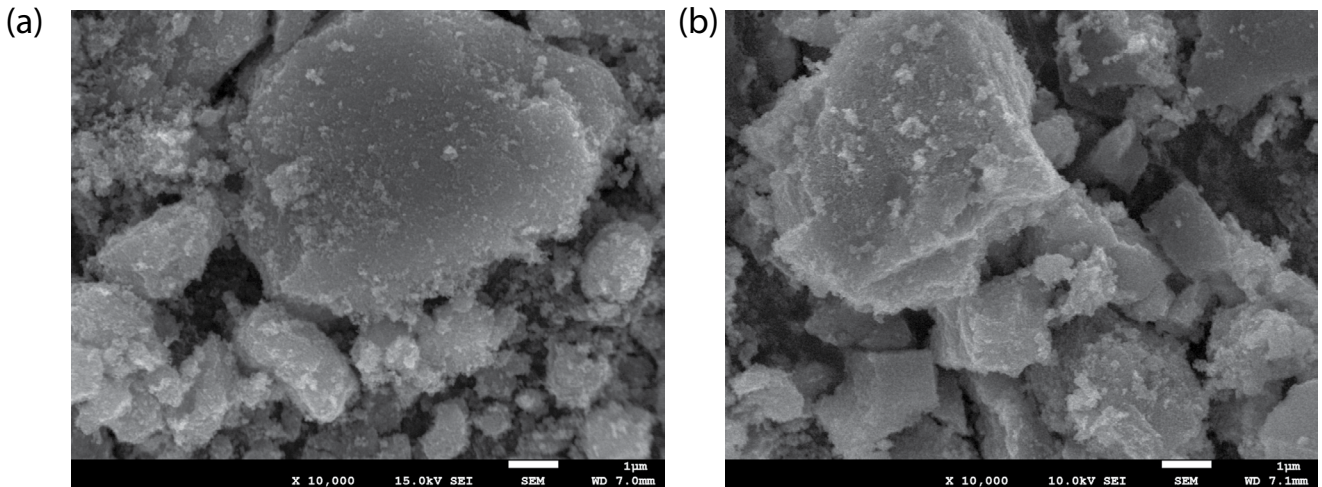


Fig. 4. SEM photograph of AC (a) and AC-MB (b).

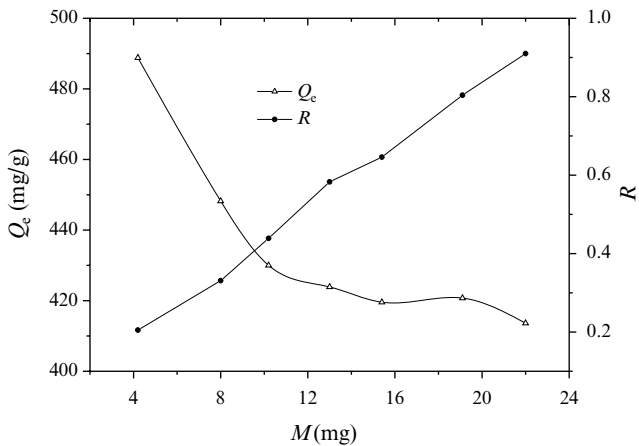


Fig. 5. Effect of AC dose on values of Q_e and R ($C_0 = 500$ mg/L; $t = 8$ h; $T = 303$ K).

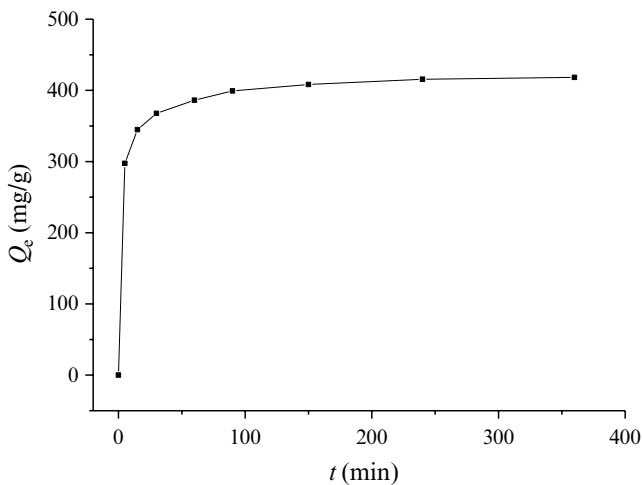


Fig. 6. Effect of contact time on adsorption quantity ($C_0 = 500$ mg/L; $T = 303$ K).

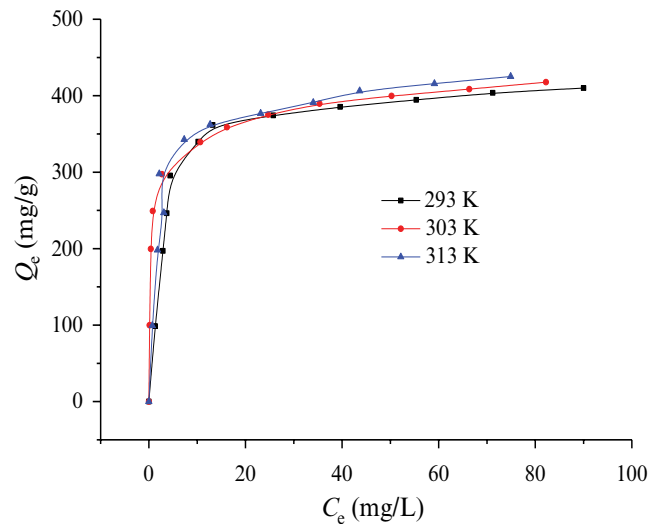


Fig. 7. Adsorption isotherms at 293, 303 and 313 K.

by four isotherm models using nonlinear regressive analysis with at least a sum of different square. The fitted parameters are in Table 2 and the fitted curves are presented in Fig. 8. Moreover, the details of the fitted coefficient listed in Table 2.

It was clearly seen from Table 2 that Langmuir and Koble–Corrigan (K–C) isotherm at 293 and 313 K owned quite high R^2 . Considering the K–C isotherm has three parameters, the costs of calculation higher than Langmuir [19]. Besides Temkin isotherm at a low range of adsorption process had a more precise tendency than K–C from Fig. 8 (303 K). By comprehensive consideration, choose Langmuir at 293 and 313 K while Temkin model at 303 K as the fitting functions ($Q_e = f_{iso}(C_e)$).

As there is more number of the acidic functional group and the solution pH of zero charge point is near 4.5, it is favor of MB adsorption at solution pH 7. So it is implied that electrostatic attraction between MB and AC is a major mechanism, also including π – π dispersion interaction.

Table 2
Parameters of adsorption isotherm models for MB onto AC at different temperatures

T/K		293	303	313
Langmuir	q_m	422 ± 9.85	387 ± 8.87	420 ± 12.1
	K_L	0.357 ± 0.0401	2.31 ± 0.379	0.584 ± 0.0884
	R^2	0.980	0.971	0.967
Freundlich	K_F	188 ± 22	230 ± 12	204 ± 20
	$1/n$	0.190 ± 0.035	0.146 ± 0.016	0.184 ± 0.030
	R^2	0.883	0.958	0.902
Temkin	A	150 ± 24	232 ± 7	182 ± 19
	B	64.7 ± 8.0	44.4 ± 2.4	61.3 ± 6.8
	R^2	0.925	0.984	0.936
Koble–Corrigan	A	90.5 ± 15.7	550 ± 63	239 ± 44
	B	0.227 ± 0.0386	1.27 ± 0.196	0.575 ± 0.104
	n	1.50 ± 0.15	0.551 ± 0.078	1.06 ± 0.23
	R^2	0.981	0.987	0.964

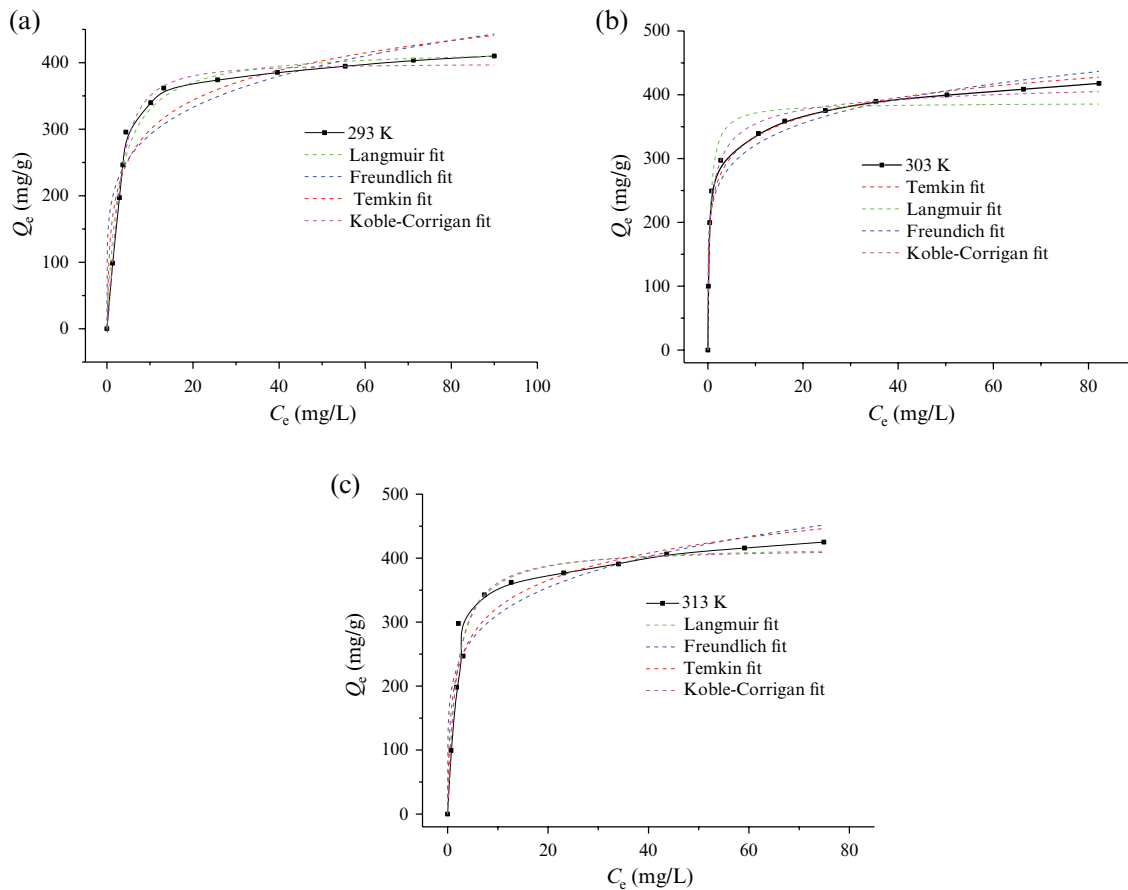


Fig. 8. Fitted curves of MB adsorption onto AC at (a) 293, (b) 303 and (c) 313 K.

3.3. Multi-stage process design analysis

3.3.1. Two-stage process batch adsorption design and calculation

Adsorption isotherms can be applied to evaluate the required adsorbent mass under known sets of initial

conditions [26]. The calculation results are shown in Fig. 9. Following the change of M_1 , the C_2 totally presented a non-linear changing tendency which had emerged a minimal value. Through the comparison between data of Fig. 9, it indicated that the two-stage batch mode could increase the final removal efficiency of MB adsorption on AC theoretically.

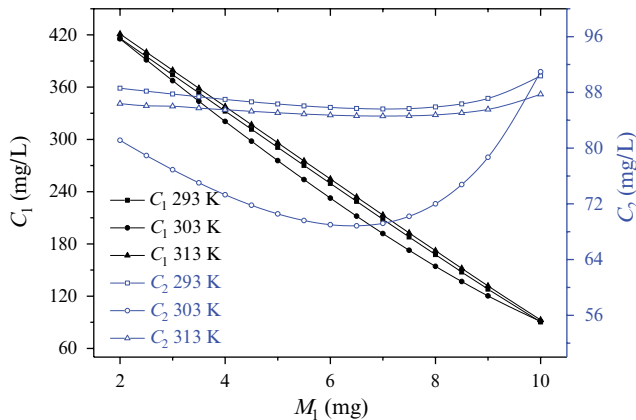


Fig. 9. Calculation results of the two-stage adsorption process at three temperatures.

Because the fitting function ($Q_e = f_{iso}(C_e)$) at 303 K differed from the functions at 293 and 313 K, the C_2 of 293 K calculation was lower than others. But generally speaking, three groups of calculations kept a similar tendency under the M_1 changing.

Comparing the calculation results of single-stage, results of two-stage and infinite multi-stage adsorption processes are listed in Table 3, the Temkin model of 303 K had a higher prediction on final results than the Langmuir model at 293 and 313 K evidently. It indicated that choosing the ideal fitting isotherm was quite significant to obtain the precise subsequent data. In addition, generally, the two-stage processes were fairly convenient and effective comparing the multi-stage adsorption process [27].

3.3.2. Two-stage batch adsorption process experiment and data contrast

The results are presented in Fig. 10. It can be seen from Fig. 10 that the developing trend of measured C_2 obeyed to the prediction of model calculation. In other words, taking into account the experimental error, the experimental results basically met the prediction of calculations. On account of fitting function distinction, the results at 293 and 313 K showed that the measured value totally was a little lower than predicted value while the measured value was fair close to predicted value at 303 K. More significantly, the real minimal value of C_2 was approximately predicted by the calculation. By arranging the amount of adsorbent

in each stage reasonably, it will be existed a point owning the maximal value of removal efficiency under the condition of a fixed adsorbent mass. For example, when the $M_1 = 7.5$ mg and $M_2 = 2.5$ mg at 293 K, the final concentration C_2 arrived at the lowest point 77 mg/L which was the approximate lowest point predicted by calculation. The absolute difference value of the lowest point was controlled within the range of 10 mg/L. Meanwhile, when the $M_1 = 10$ mg and $M_2 = 0$ at 293 K, that means this was the single batch adsorption process, and the final concentration C_2 was close to 90 mg/L. It indicated that the two-stage batch adsorption process performed higher effectiveness than the single batch adsorption process and the calculation value of designing models had a remarkable predicted effect towards measure the value of the real practical operation.

3.3.3. Adsorbent amount optimization for one certain removal efficiency in a two-stage process

The results of adsorbent amount optimization are shown in Fig. 11 at a given value of R . It was noticed that the higher removal efficiency was required, the more obvious did the advantage of two-stage batch adsorption models. For pursuing high removal in the adsorption, the consumption of adsorbent was usually quite large in the single-stage batch adsorption process. However, multi-stage batch adsorption was fairly helpful in reducing the cost of the adsorbent. Taking a group data in Table 4 as the example, in order to get the requirement of 99% MB removal efficiency onto AC at 293 K, the two-stage batch process was competent to save 30% amount of AC than single-stage batch process approximately. Even if the multi-stage process could approach approximately save 34%, the complex operation would cost a lot. Therefore, the preferable strategy was the two-stage adsorption from many aspects of considerations [28].

4. Conclusion

The equilibrium research showed that the Langmuir isotherm model was fitted well at 293 and 313 K while the Temkin isotherm model has better fitness at 303 K for the adsorption experiment of MB onto AC. The two-stage adsorption model and multi-stage adsorption model were established and applied for the result predictions of adsorption processes at 293, 303 and 313 K. The predictions showed the two-stage adsorption model performed efficiently and promoted the utilization of adsorbent at different temperatures. Besides that, the practical results of two-stage

Table 3

Calculation results of single-stage, two-stage and infinite multi-stage adsorption process in the initial experimental conditions ($C_0 = 500$ mg/L; $V = 10$ mL and $M = 10$ mg)

Batch mode	Removal efficiency	293 K	303 K	313 K
Single-stage	R	0.819	0.848	0.825
	R_1	0.583	0.606	0.542
Two-stage	R_2	0.245	0.286	0.288
	R_{total}	0.829	0.892	0.831
Infinite multi-stage	R_{Max}	0.835	0.939	0.835

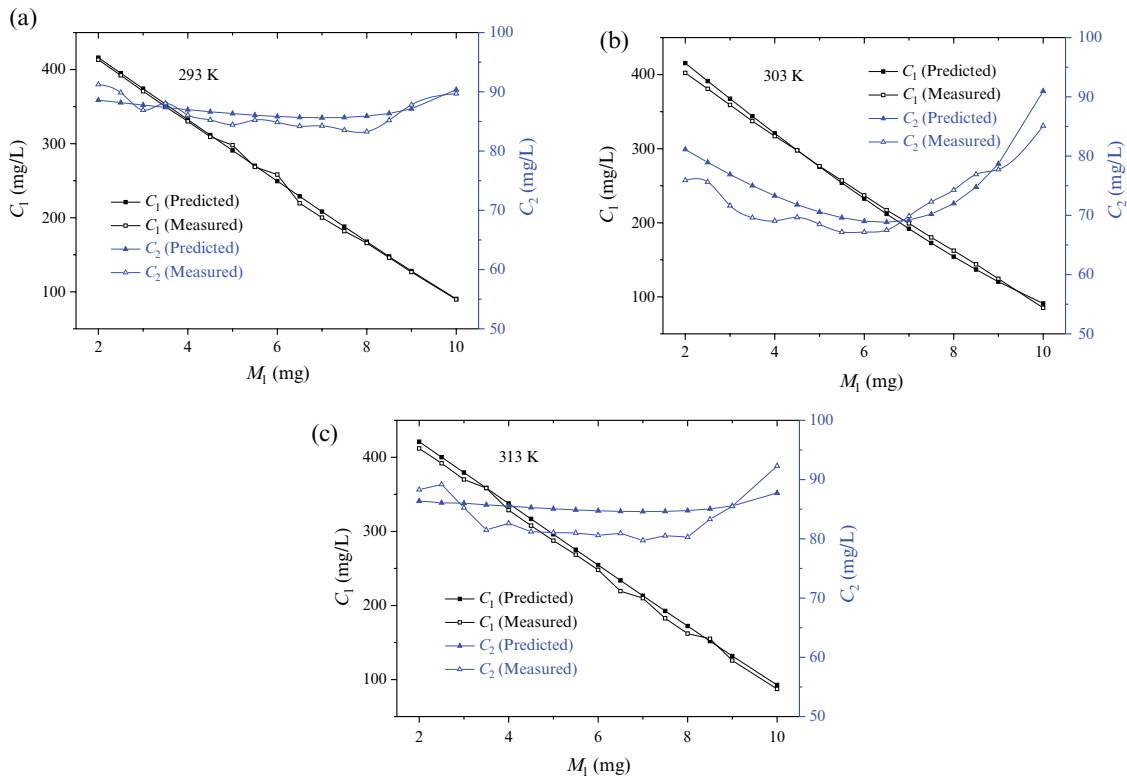


Fig. 10. Comparison of results between calculation and experiments in a two-stage process (a) 293, (b) 303 and (c) 313 K.

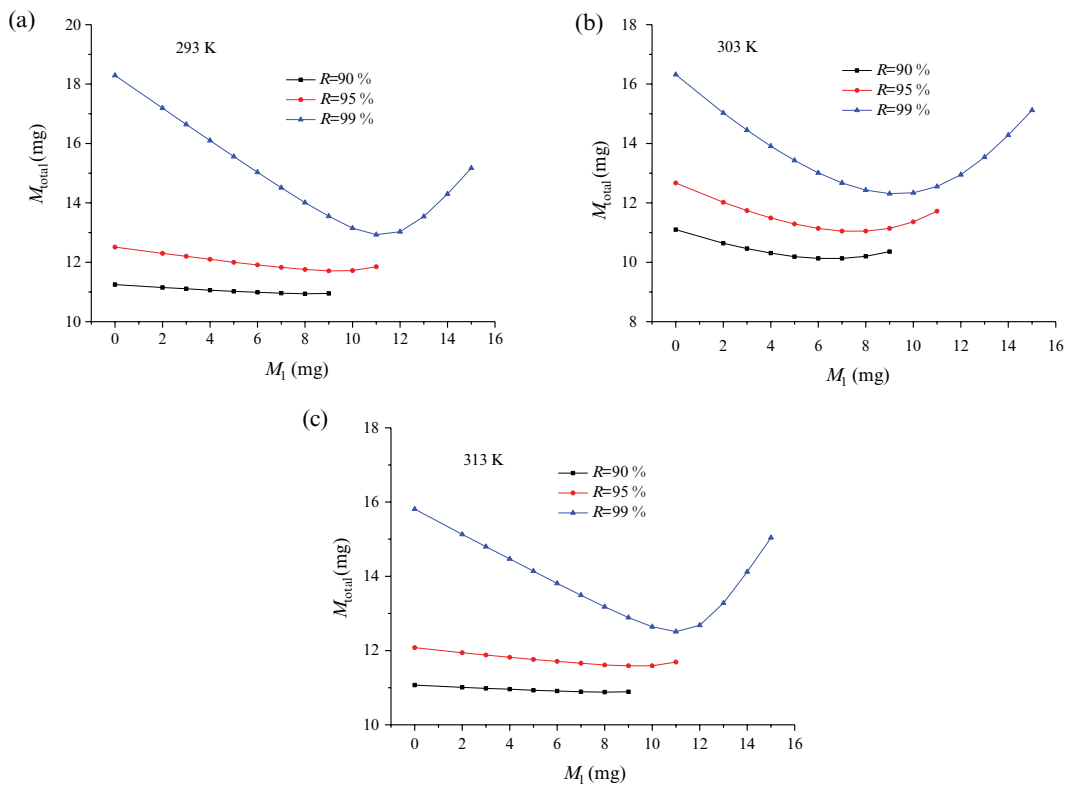


Fig. 11. The M follow M_1 changing in condition of 90%, 95% and 99% removal efficiency (a) 293, (b) 303 and (c) 313 K.

Table 4
Comparison total adsorbent consumption among single-stage, two-stage and infinite multi-stage processes in conditions of 90%, 95% and 99% removal efficiency

R	Batch mode	Mass (mg)	293 K	303 K	313 K
90%	Single-stage	M	11.25	11.10	11.07
		M_1	8	6	8
	Two-stage	M_2	2.94	4.13	2.88
		M_{total}	10.94	10.13	10.88
	Multi-stage	M_{min}	10.81	9.51	10.80
		Single-stage	M	12.51	12.67
95%	Single-stage	M_1	9	7	9
		M_2	2.71	4.05	2.59
	Two-stage	M_{total}	11.71	11.05	11.59
		M_{min}	11.45	10.15	11.42
	Multi-stage	M	18.29	16.32	15.81
		Single-stage	M_1	11	9
99%	Single-stage	M_2	1.93	3.31	1.51
		M_{total}	12.93	12.31	12.51
	Two-stage	M_{min}	12.03	10.73	11.96
		Multi-stage	M_{min}	12.03	10.73

adsorption operation were quite close to the prediction of models which proved the reliability of the two-stage adsorption models. In the end, from the view of reducing the adsorbent consumption aimed at a fixed removal efficiency of MB, the two-stage adsorption model had an impressive effect on the adsorbent saving. It was particularly applicable for optimizing the use of adsorbent to save capital investment costs and especially when the requirement for dye removal efficiency was very high.

Acknowledgment

This work was supported in part by the Key Scientific Research Project in Universities of Henan Province (19A150048).

References

- [1] Y.B. Zhou, J. Lu, Y. Zhou, Y.D. Liu, Recent advances for dyes removal using novel adsorbents: a review, *Environ. Pollut.*, 252 (2019) 352–365.
- [2] J.W. Liu, J.G. Jiang, Y. Meng, A. Aihemaiti, Y.W. Xu, H.L. Xiang, Y.C. Gao, X.J. Chen, Preparation, environmental application and prospect of biochar-supported metal nanoparticles: a review, *J. Hazard. Mater.*, 388 (2020) 122026.
- [3] X. Xu, B.Y. Gao, B. Jin, Q.Y. Yue, Removal of anionic pollutants from liquids by biomass materials: a review, *J. Mol. Liq.*, 215 (2016) 565–595.
- [4] A. Talaiekhozani, S. Rezaia, Application of photosynthetic bacteria for removal of heavy metals, macro-pollutants and dye from wastewater: a review, *J. Water Process Eng.*, 19 (2017) 312–321.
- [5] A. Bhatnagar, W. Hogland, M. Marques, M. Sillanpää, An overview of the modification methods of activated carbon for its water treatment applications, *Chem. Eng. J.*, 219 (2013) 499–511.
- [6] F. Mbarki, T. Selmi, A. Kesraoui, M. Seffen, P. Gadonneix, A. Celzard, V. Fierro, Hydrothermal pre-treatment, an efficient tool to improve activated carbon performances, *Ind. Crops Prod.*, 140 (2019) 111717.
- [7] T. Zhou, W.Z. Lu, L.F. Liu, H.M. Zhu, Y.B. Jiao, S.S. Zhang, R.P. Han, Effective adsorption of light green anionic dye from solution by CPB modified peanut in column mode, *J. Mol. Liq.*, 211 (2015) 909–914.
- [8] B.L. Zhao, W. Xiao, Y. Shang, H.M. Zhu, R.P. Han, Adsorption of light green anionic dye using cationic surfactant-modified peanut husk in batch mode, *Arabian J. Chem.*, 10 (2017) S3595–S3602.
- [9] S.S. Chen, K. Wen, X.T. Zhang, R.Z. Zhang, R.P. Han, Adsorption of neutral red onto MIL-100(Fe) from solution: characterization, equilibrium, kinetics, thermodynamics and process design, *Desal. Water Treat.*, 177 (2020) 197–208.
- [10] Q. Li, Q.Y. Yue, Y. Su, B.Y. Gao, Equilibrium and a two-stage batch adsorber design for reactive or disperse dye removal to minimize adsorbent amount, *Bioresour. Technol.*, 102 (2011) 5290–5296.
- [11] M. Özacar, Contact time optimization of two-stage batch adsorber design using second-order kinetic model for the adsorption of phosphate onto alunite, *J. Hazard. Mater.*, 137 (2006) 218–225.
- [12] Y.C. Rong, R.P. Han, Adsorption of *p*-chlorophenol and *p*-nitrophenol in single and binary systems from solution using magnetic activated carbon, *Korean J. Chem. Eng.*, 36 (2019) 942–953.
- [13] J.Y. Song, W.H. Zou, Y.Y. Bian, F.Y. Su, R.P. Han, Adsorption characteristics of methylene blue by peanut husk in batch and column modes, *Desalination*, 265 (2011) 119–125.
- [14] W.L. Wang, Y.Y. Du, M.Y. Liu, M.M. Yang, R.P. Han, Adsorption of congo red from solution using chitosan modified carbon nanotubes, *Desal. Water Treat.*, 156 (2019) 96–105.
- [15] M. Özacar, İ. Ayhan Şengül, A two stage batch adsorber design for methylene blue removal to minimize contact time, *J. Environ. Manage.*, 80 (2006) 372–379.
- [16] Y. Liu, Y.-J. Liu, Biosorption isotherms, kinetics and thermodynamics, *Sep. Purif. Technol.*, 61 (2008) 229–242.
- [17] R.D. Zhang, J.H. Zhang, X.N. Zhang, C.C. Dou, R.P. Han, Adsorption of Congo red from aqueous solutions using cationic surfactant modified wheat straw in batch mode: kinetic and equilibrium study, *J. Taiwan Inst. Chem. Eng.*, 45 (2014) 2578–2583.
- [18] S.S. Tahir, N. Rauf, Removal of a cationic dye from aqueous solutions by adsorption onto bentonite clay, *Chemosphere*, 63 (2006) 1842–1848.
- [19] B.H. Foo, K.Y. Hameed, Insights into the modeling of adsorption isotherm systems, *Chem. Eng. J.*, 156 (2010) 2–10.
- [20] C.S.T. Araújo, I.L.S. Almeida, H.C. Rezende, S.M.L.O. Marcionilio, J.J.L. Léon, T.N. de Matos, Elucidation of mechanism involved in adsorption of Pb(II) onto lobeira fruit (*Solanum lycocarpum*) using Langmuir, Freundlich and Temkin isotherms, *Microchem. J.*, 137 (2018) 348–354.
- [21] A. Ladshaw, S. Yiacoumi, C. Tsouris, D. DePaoli, Generalized gas–solid adsorption modeling: single-component equilibria, *Fluid Phase Equilib.*, 388 (2015) 169–181.
- [22] J.U. Keller, J.D. Popernack, R. Staudt, A generalization of Langmuir’s adsorption isotherm to molecules with interaction, *Adsorpt. Sci. Technol.*, 20 (2000) 336–340.
- [23] K.C. Ng, M. Burhan, M.W. Shahzad, A.B. Ismail, A universal isotherm model to capture adsorption uptake and energy distribution of porous heterogeneous surface, *Sci. Rep.*, 7 (2017), <https://doi.org/10.1038/s41598-017-11156-6>.
- [24] Y.C. Rong, H. Li, L.H. Xiao, Q. Wang, Y.Y. Hu, S.S. Zhang, R.P. Han, Adsorption of malachite green dye from solution by magnetic activated carbon in batch mode, *Desal. Water Treat.*, 106 (2018) 273–284.
- [25] Y.B. Jiao, D.L. Han, Y.Z. Lu, Y.C. Rong, L.Y. Fang, Y.L. Liu, R.P. Han, Characterization of pine-sawdust pyrolytic char activated by phosphoric acid through microwave irradiation and adsorption property toward CDNB in batch mode, *Desal. Water Treat.*, 77 (2017) 247–255.
- [26] H.-K. Chung, W.-H. Kim, J.W. Park, J.W. Cho, T.-Y. Jeong, P.-K. Park, Application of Langmuir and Freundlich isotherms to predict adsorbate removal efficiency or required amount of adsorbent, *J. Ind. Eng. Chem.*, 28 (2015) 241–246.

- [27] L. Li, J. Iqbal, Y. Zhu, F. Wang, F.Y. Zhang, W.C. Chen, T. Wu, Y.P. Du, Chitosan/Al₂O₃-HA nanocomposite beads for efficient removal of estradiol and chrysoidin from aqueous solution, *Int. J. Biol. Macromol.*, 145 (2020) 686–693.
- [28] J. Iqbal, N.S. Shah, M. Sayed, M. Imran, N. Muhammad, F.M. Howari, S.A. Alkhoori, J.A. Khan, Z. Ul Haq Khan, A. Bhatnagar, K. Polychronopoulou, I. Ismail, M.A. Haija, Synergistic effects of activated carbon and nano-zerovalent copper on the performance of hydroxyapatite-alginate beads for the removal of As³⁺ from aqueous solution, *J. Cleaner Prod.*, 235 (2019) 875–886.